Global Land Monsoon Precipitation Changes in CMIP6 Projections

Ziming Chen[1, 2], Tianjun Zhou[1, 2, 3], Lixia Zhang[1, 3], Xiaolong Chen[1, 3], Wenxia Zhang[1], Jie Jiang[1, 2]

1. State Key Laboratory of Numerical Modeling for Atmospheric Sciences and Geophysical Fluid Dynamics, Institute of Atmospheric Physics, Chinese Academy of Sciences, Beijing, China , 100029
2. University of the Chinese Academy of Sciences, Beijing, China, 100049
3. CAS Center for Excellence in Tibetan Plateau Earth Sciences, Chinese Academy of Sciences (CAS), Beijing, China

1. Introduction

- About two third of global population relies on the water resource from global monsoon (GM) summer precipitation. The GM system is sensitive to global warming. Thus, understanding and predicting the changes of GM are critically important.
- The Coupled Model Intercomparison Project Phase 6 (CMIP6) has designed new scenarios called Shared Socioeconomic Pathway (SSP) 1–2.6, SSP2–4.5, SSP3–7.0, and SSP5–8.5[2,3]. Climate change mitigation and adaptation need the projection under these new scenarios in different terms.
- **Question:**
  - **(1) What are the future changes in global land monsoon (GLM) precipitation under different CMIP6 scenarios in different periods?**
  - **(2) What are the mechanisms for the changes and what are the sources of uncertainty in GLM precipitation in different projection terms?**
  - **(3) Whether a uniform warming could reduce or eliminate the uncertainty of GLM precipitation projection?**

2. Data and Methods

- Data:
  - Historical simulation and projection under SSP1-2.6, SSP2-4.5, SSP3-7.0 and SSP5-8.5 scenarios of 19 CMIP6 models[2,3].
  - AMIP and AMIP-p4K experiment of nine CMIP6 models[4].
- GLM domain:
  - The land area where the precipitation difference between the local summer (Northern Hemisphere (NH): MJJAS; Southern Hemisphere (SH): NDJFM) and winter is larger than 2.0 mm day^{-1}, and local summer precipitation exceeds 55% of the annual total precipitation[5].
- Projected uncertainty:
  - The spread from 10th to 90th percentile across models.
- Moisture budget diagnosis:
  - $P' = E' - \langle\overline{\overrightarrow{u_h}}\cdot\nabla q'\rangle - \langle\overrightarrow{u_h}'\cdot\nabla\bar{q}\rangle - \langle\bar{\omega}\partial_p q'\rangle - \langle\omega'\partial_p\bar{q}\rangle + NL + Residual$, (1)
  - $TH = -\langle\bar{\omega}\partial_p q'\rangle, DY = -\langle\omega'\partial_p\bar{q}\rangle, NL = -\langle\overrightarrow{u_h}'\cdot\nabla q'\rangle - \langle\omega'\partial_p q'\rangle$, (2)

Model	Institute/Country	Lat x Lon	The Number of Realizations
BCC-CSM2-MR	BCC-CMA/China	160 x 320	1
CAMS-CSM1-0	CAMS-CMA/China	160 x 320	1
CNRM-CM6-1	CNRM-CERFACS/France	128 x 256	1
CNRM-ESM2-1	CNRM-CERFACS/France	128 x 256	1
CanESM5	CCCMA/Canada	64 x 128	6
EC-Earth3	EC-Earth-Consortium/EU	256 x 512	1
EC-Earth3-Veg	EC-Earth-Consortium/EU	256 x 512	1
FGOALS-f3-L	LASG-IAP/China	180 x 360	1
FGOALS-g3	LASG-IAP/China	90 x 180	1
GFDL-CM4	GFDL-NOAA/USA	180 x 360	1
GFDL-ESM4	GFDL-NOAA/USA	180 x 360	1
INM-CM5-0	INM/Russia	120 x 180	1
IPSL-CM6A-LR	IPSL/France	143 x 144	6
MCM-UA-1-0	UA/USA	80 x 96	1
MIROC6	MIROC/Japan	128 x 256	1
MIROC-ES2L	MIROC/Japan	64 x 128	1
MRI-ESM2-0	MRI/Japan	96 x 192	1
NESM3	NUIST/China	96 x 192	1
UKESM1-0-LL	MOHC/UK	144 x 192	5

3. Precipitation Changes in the Projection

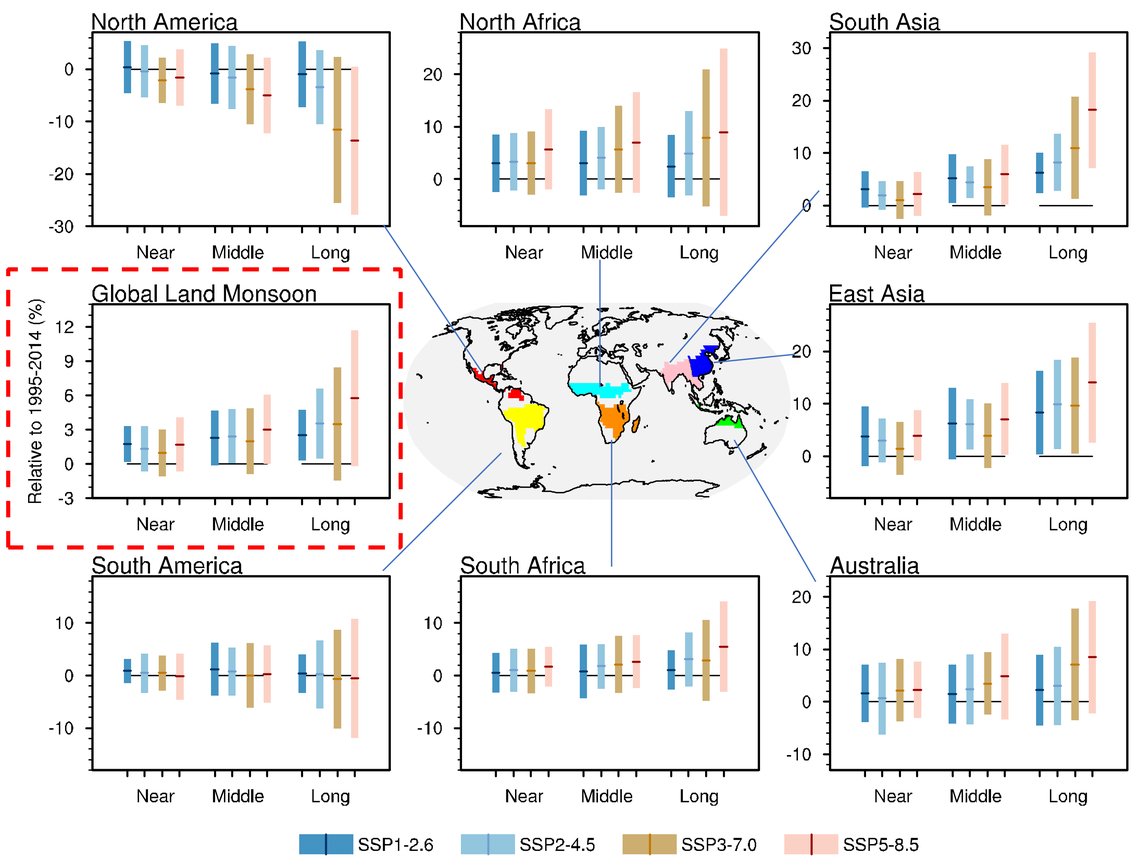

Figure 3.1. Summer precipitation changes of global land monsoon (red box) and each submonsoon region in near-term (2021–2040), midterm (2041–2060), and long-term (2080–2099) projections under SSP1–2.6, SSP2–4.5, SSP3–7.0, and SSP5–8.5 scenarios, relative to the climatology in 1995–2014 (unit: %). The thick lines represent the CMIP6 mult-imodel ensemble, while the bars indicate the 10th to 90th ranges.

- The GLM summer precipitation is projected to increase by 1.76 ± 1.57% (2.54 ± 2.22%), 1.33 ± 1.97% (3.52 ± 3.05%), 0.96 ± 2.04% (3.51 ± 4.97%), and 1.71 ± 2.38% (5.75 ± 5.92%) in the near (long) term under SSP1–2.6, SSP2–4.5, SSP3–7.0, and SSP5–8.5, respectively.
- Regionally, the Asian summer monsoon precipitation will increase robustly in the long term of 4 scenarios (6.21%~18.21%), while the American monsoon precipitation will reduce (-0.95%~-13.62%).
- The uncertainty in GLM precipitation is the largest in SSP5–8.5 long-term projection, while the uncertainty of submonsoon precipitation is larger than that in GLM precipitation.

4. Thermodynamic (TH) and Dynamic (DY) Contribution

Monsoon Precipitation Increases: Water Vapor Contribution

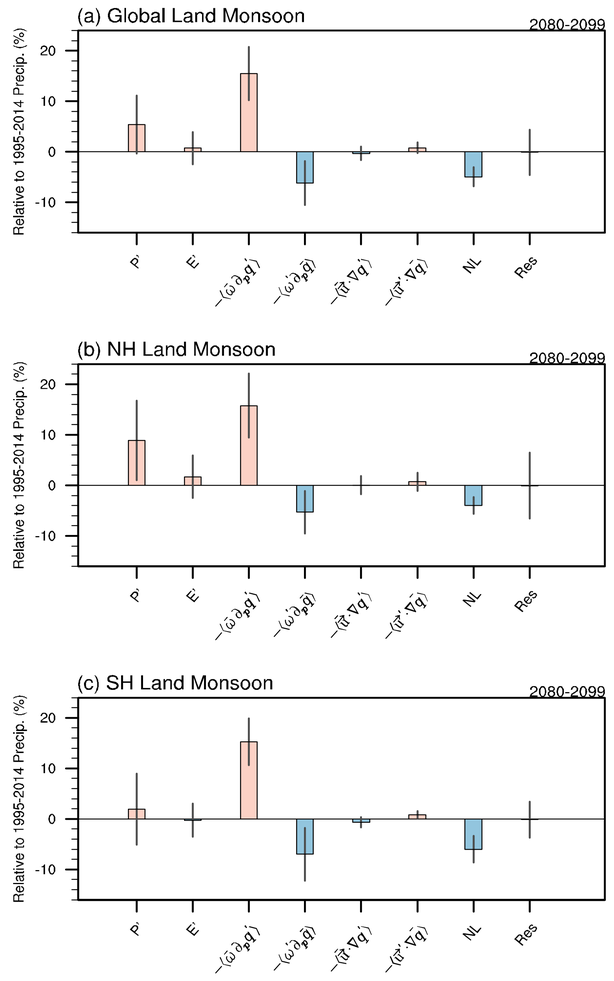

- Precipitation increase over GLM region is dominated by the increase of water vapor (TH, $-\langle\bar{\omega}\partial_p q'\rangle$), while the effect of circulation changes (DY, $-\langle\omega'\partial_p\bar{q}\rangle$) and NL terms partly offset the increase in precipitation.
- Regionally, the changes over NH land monsoon regions are similar to that of GLM and dominated by the increase of water vapor, except for the North American monsoon region where the effects of circulation changes and NL term cause the decline of precipitation.
- The enhancement of precipitation over SH land monsoon regions is moderate since the negative contribution from DY and NL is stronger than that in NH.

Figure 4.1. The changes of moisture budget terms in the long term under SSP5–8.5 scenario averaged over the (a) global land monsoon domain, (b) Northern Hemisphere (NH) land monsoon, and (c) Southern Hemisphere (SH) land monsoon, relative to the summer mean precipitation in 1995–2014. The bars represent the multi-model ensemble, while the vertical lines indicate the range of 10th to 90th.

Monsoon Precipitation Uncertainty: Contribution of Circulation Patterns

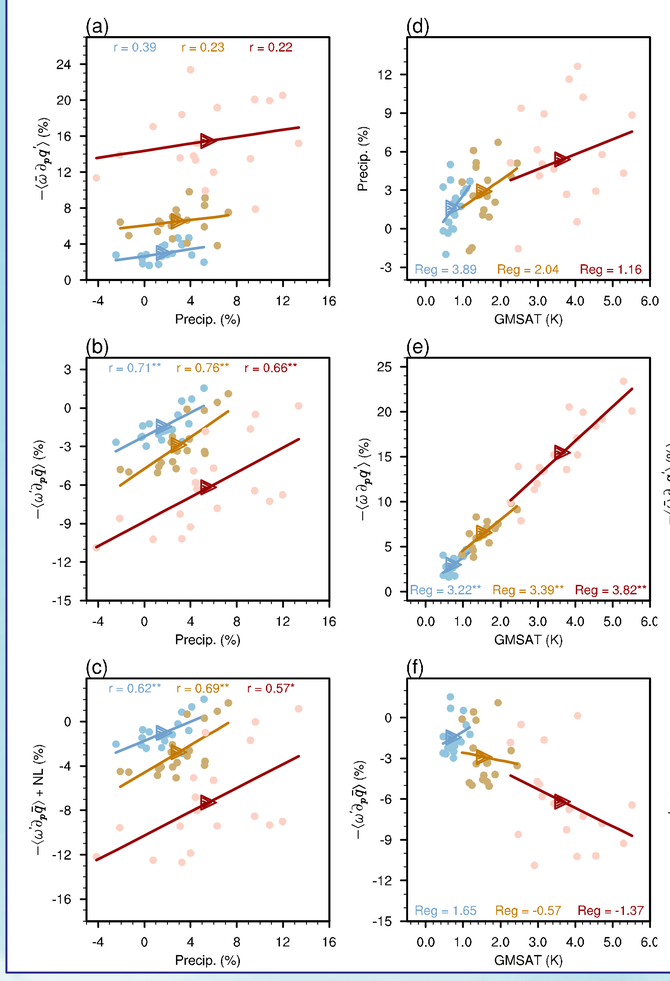

- The spread of CMIP6 models in the midterm and long-term projections is dominated by the uncertainty of circulation (DY) rather than water vapor increases (TH).
- Only a small part of the uncertainty can be explained by the global mean air temperature increases, and the source of circulation uncertainty can be partly explained by model-dependent response to the uniform SST warming.

Figure 4.2. Relationship between precipitation changes and TH, DY, global mean surface air temperature increase in SSP5-8.5 (a-f) and AMIP-p4K (g-h) experiment. Units: %

5. Summary

- The precipitation over the GLM region will increase significantly under the four CMIP6 scenarios. The precipitation changes in near term and midterm are comparable across the four scenarios, while the enhancement is largest under SSP5-8.5 long-term projection (5.75%±5.92%). The projection uncertainty increases with time except for SSP1–2.6.
- The enhancement in precipitation is caused by the TH term with increased moisture, while partly offset by the DY term to weakened atmospheric circulation. While the projected GLM precipitation increases are dominated by the TH term, the uncertainty is induced by the DY term in the midterm and long-term projection.
- The uncertainty in the circulation changes is still evident under uniform SST warming. The model-dependent response to the uniform SST warming partly explains the uncertainty in circulation changes.

Reference:

[1] Chen, Z., Zhou, T., Zhang, L., et al. (2020), Global Land Monsoon Precipitation Changes in CMIP6 Projections. Geophysical Research Letters, 47(14). doi:10.1029/2019gl086902.

Other References:

[2] Eyring, V., Bony, S., Meehl, G. A., et al. (2016), Overview of the Coupled Model Intercomparison Project Phase 6 (CMIP6) experimental design and organization. Geoscientific Model Development, 9(5), 1937-1958. doi:10.5194/gmd-9-1937-2016.

[3] O'Neill, B. C., et al. (2016), The Scenario Model Intercomparison Project (ScenarioMIP) for CMIP6. Geoscientific Model Development, 9(9), 3461-3482. doi:10.5194/gmd-9-3461-2016.

[4] Webb, M. J., et al. (2017), The Cloud Feedback Model Intercomparison Project (CFMIP) contribution to CMIP6. Geoscientific Model Development, 10(1), 359-384. doi:10.5194/gmd-10-359-2017.

[5] Wang, B., Liu, J., Kim, H.-J., et al.. (2012), Recent change of the global monsoon precipitation (1979–2008). Climate Dynamics, 39(5), 1123-1135. doi:10.1007/s00382-011-1266-z.